

Nuclear fragmentation characteristics from isotopic spin dependent lattice-gas model

S. K. Samaddar^{1,2} and S. Das Gupta¹

¹Physics Department, McGill University, 3600 University St., Montréal, Québec, Canada H3A 2T8

²Saha Institute of Nuclear Physics, 1/AF Bidhannagar, Calcutta 700064, India

(Received 4 November 1999; published 16 February 2000)

An isotopic spin dependent lattice-gas model is employed to investigate several characteristics of nuclear fragmentation observed in intermediate energy heavy ion collisions. In addition to the isotopic spin dependent nearest neighbor interaction the Coulomb interaction between protons, expected to be important for heavy systems, is also taken into account. The model is used to calculate a number of fragmentation observables with special emphasis on the dependence of particle emission on the isospin content of the disassembling system.

PACS number(s): 25.70.Pq, 24.10.Pa, 64.60.My

I. INTRODUCTION

In this paper we consider several applications of an isospin dependent lattice-gas model. The model allows direct calculation of observables as well as computation of the equation of state. In the early version of the lattice-gas model (LGM) [1,2] for nuclear multifragmentation no distinction was made between neutron-neutron bonds (ϵ_{nn}), proton-proton bonds (ϵ_{pp}), and neutron-proton bonds (ϵ_{np}). The model was subsequently modified to allow for differences in the interaction between like particles and unlike particles [3,4] ($\epsilon_{nn} = \epsilon_{pp} \neq \epsilon_{np}$). In some of the calculations the Coulomb interaction between protons was also taken into account [3].

In this paper we show that (a) the isospin dependent lattice-gas model reproduces the liquid drop binding energies fairly well (Sec. III), (b) for large systems both the isotopic spin dependence and Coulomb interaction between protons should be included (Sec. IV), and (c) the model reasonably well reproduces data of experimentally studied $^{112}\text{Sn} + ^{112}\text{Sn}$ and $^{124}\text{Sn} + ^{124}\text{Sn}$ reactions (Sec. V). These experimental results strongly highlight the isotopic spin dependence of the model and hence provide an important test of the model. But first, in the next section, we describe the prescription used to do the calculations.

II. CLUSTERIZATION FORMULA

We provide an outline here of how clusters are computed. Let us first ignore the Coulomb interaction and for brevity assume that there is only one kind of bond ϵ . We put, using the METROPOLIS algorithm [5], A nucleons in N_s lattice sites at a given temperature T . Here $A/N_s = \rho/\rho_0$ where ρ is the freeze-out density and ρ_0 is normal nuclear density. Once the nucleons have been put in lattice sites, each is ascribed a momentum by Monte Carlo sampling the Maxwell-Boltzmann distribution at the given temperature T . One is now ready to obtain the cluster distribution for this configuration called an event.

In a particular configuration there may be some isolated nucleons. They do not have any interacting partners and are therefore singles. The next case is when there is a cluster of two nucleons which are nearest neighbors of each other. Clearly this will form a bound cluster if the kinetic energy of

the relative motion is insufficient to overcome the attraction between the nucleons, i.e., $p_r^2(1,2)/2\mu + \epsilon < 0$. Here $\vec{p}_r(1,2) = \frac{1}{2}(\vec{p}_1 - \vec{p}_2)$ and $\mu = m/2$ ($m = \text{mass of one nucleon}$).

It turns out this prescription which is rigorously correct for a cluster of two is also expected to work *statistically* for larger clusters. That is, we can formulate the rule that independent of other neighbors two nearest neighbors form part of the same cluster if the relative kinetic energy of the two is insufficient to overcome their attraction. It is obvious that this reduces the many body problem of recognizing a cluster of many nucleons into a sum of independent two-body problems. For brevity we will call this the Pan-Das Gupta (PD) prescription [1]. To see why this works *statistically* even though not individually let us specifically consider a three-body cluster. The generalization to higher clusters can be done.

For three-particle clusters the nearest neighbors are either linear or L shaped. In either case there is only one particle which has two bonds (label this particle number 2) and two others (label them 1 and 3) which have one bond each. According to our ‘‘simple’’ prescription this will form a three-body cluster if $p_r^2(1,2)/2\mu + \epsilon < 0$ and $p_r^2(2,3)/2\mu + \epsilon < 0$. To check if particle 3 is part of a three-body cluster (similar arguments will be needed for particles 1 and 2) we should instead verify if $p_r^2(12,3)/2\tilde{\mu} + \epsilon < 0$. Here $\vec{p}_r(12,3)$ is the relative momentum between the center of mass of (1+2) and 3; $\tilde{\mu} = (2/3)m$ is the reduced mass for this relative motion. Thus there may be cases where with our simple prescription we get a three-body cluster though in reality the third one will separate, but also there will be cases where with our prescription we will deem that the third one will separate whereas in reality it stays attached. Statistically overestimation will cancel out underestimation because for a Maxwell-Boltzmann distribution all relative motions are also Maxwellian. That is, in Monte Carlo simulations, $p_r^2(12,3)/2\tilde{\mu}$ will be as many times below the value of $-\epsilon$ as $p_r^2(1,2)/2\mu$ will be.

The same argument applies to particle 1. For particle 2, it can be verified that if $p_r^2(1,2)/2\mu + \epsilon < 0$ and $p_r^2(2,3)/2\mu + \epsilon < 0$, then $p_r^2(13,2)/2\tilde{\mu} + 2\epsilon < 0$ is always satisfied.

The generalization to more complicated cases is straightforward. It only hinges on the fact that with a Maxwell-

Boltzmann distribution relative motions are also Maxwellian.

This shows that in a statistical generation of different composites with this prescription we do not need to worry about subsequent evaporation as one needs to do in some other models [6]. Evaporation was already taken into account when we applied the formula. One does not take the size of the cluster to be given by just the number of nucleons which are connected to each other through nearest neighbor interactions. Some of these will fly away. The rest that remain and are counted are particle stable.

To include isospin dependence we use $\epsilon_{pp} = \epsilon_{nn} \neq \epsilon_{np}$. The METROPOLIS algorithm easily handles this distinction. A switch is attempted between (a) occupied and unoccupied sites and (b) between occupied neutron and proton sites. When we want to include the Coulomb term we include the change in the Coulomb energy when the switch is attempted. Once the particles are put in the lattice sites we just use the PD rule to calculate clusters. The Coulomb effect is neglected when clusters are computed. This is different from an earlier prescription that was adopted [3]. In that work to find the effect of the Coulomb interaction the authors (a) included the Coulomb interaction when doing the METROPOLIS algorithm and (b) propagated the nucleons after initialization by classical dynamics (just as in molecular dynamics calculations). In the propagation they used the Coulomb and a short range nuclear force (such as would justify the nearest neighbor interaction). After the molecular dynamics calculations, which were continued until asymptotic times, clusters could be unambiguously identified. We find that at least for the chagres that are encountered in heavy ion collisions this is not necessary. Including the Coulomb interaction in the METROPOLIS algorithm followed by the PD rule produces very similar results. This is a big saving in computer time.

III. EMPIRICAL MASS FORMULA AND THE ISOSPIN DEPENDENT LATTICE-GAS MODEL

In this section we show how the parameters ϵ_{np} and $\epsilon_{nn} = \epsilon_{pp}$ are chosen. Clearly the like particle bond cannot be attractive as this will produce bound dineutrons and diprotons; ϵ_{np} has to be set at -5.33 MeV so that nuclear matter has a binding energy of 16 MeV per nucleon (at zero temperature neutrons and protons will occupy alternate sites; thus the bonds are only between unlike particles). We may try to fix the value of ϵ_{nn} by a ‘‘best’’ fit to the symmetry energy for medium to heavy mass nuclei. Of course nuclear binding energies also have a surface tension term, but once we fix ϵ_{nn} from symmetry energy considerations, we have no free parameter left.

We calculate the binding energies for several nuclei in the mass range $16 \leq A \leq 252$, taking $\epsilon_{nn} = 0$. The usual METROPOLIS sampling technique [5] for event generation at finite temperature is readily adaptable to the case $T \rightarrow 0$ which then produces the ground state. The ground state energies for a number of nuclei so obtained are fitted to a simple liquid-drop model mass formula [7] given by

$$E/A = -a_v(1 - \kappa I^2) + a_s(1 - \kappa I^2)A^{-1/3} + a_c \frac{Z^2}{A^{4/3}}. \quad (3.1)$$

TABLE I. Calculated, fitted, and experimental B/A .

System	Calculated B/A	Fitted B/A	Expt. B/A
¹⁶ O	8.505	8.452	7.976
²⁷ Al	8.899	9.064	8.331
⁴⁰ Ca	9.169	9.137	8.562
⁵⁶ Fe	9.455	9.321	8.790
⁶⁴ Zn	9.304	9.269	8.736
⁹⁰ Zr	9.067	9.124	8.710
¹¹⁴ Sn	8.839	8.903	8.523
¹⁵⁰ Sm	8.589	8.496	8.244
¹⁹⁷ Au	8.039	8.063	7.915
²⁰⁸ Pb	7.826	7.940	7.867
²³⁰ Th	7.803	7.737	7.631
²³⁸ U	7.702	7.649	7.635
²⁵² Cf	7.501	7.539	7.465

Here $I = (N - Z)/A$, is the neutron-proton asymmetry of the nucleus. This mass formula contains four parameters, namely, a_v , a_s , a_c , and κ . The volume energy coefficient a_v has already been fixed at 16 MeV through the choice of ϵ_{np} . The remaining three parameters are obtained from a least-squares fit to the calculated ground state energies. The per particle binding energies obtained in the LGM, their fitted values obtained from the mass formula, and the experimental binding energies for a number of nuclei are shown in Table I. It is seen that the fitted values are within 1% of their actual calculated values. This indicates that the LGM binding energies closely follow a liquid-drop mass formula. Comparison of the calculated binding energies with the experimental ones shows that for heavy nuclei they agree within 1% which, we think, is an excellent agreement, keeping in mind the simplicity of the LGM. However, for the relatively lighter nuclei the deviations in some cases are as high as 10%. The liquid-drop model parameters obtained from the least-squares fit to the calculated LGM energies and the corresponding phenomenological values [7] are listed in Table II. We note that the asymmetry energy coefficient κ in the LGM is somewhat larger compared to the phenomenological one. A lower value for κ can be obtained only by making ϵ_{nn} negative. This is not permitted as then unphysical clusters like dineutrons or diprotons would be produced as mentioned earlier. So we fix the value of ϵ_{nn} at zero. Before leaving this section we would like to make a comment on the surface energy coefficient a_s . It can be shown that for a number of nucleons equal to the number of lattice points ($A = N_s$) the number of missing bonds at the surface is $3A^{2/3}$. For a symmetric nucleus ($N = Z$) the surface energy then becomes $3\epsilon_{np}A^{2/3}$, giving $a_s = 16.0$ MeV. It is seen from Table II that

TABLE II. Lattice-gas and phenomenological liquid-drop model parameters.

Model	a_v	a_s	κ	a_c
Lattice-gas	15.99	16.03	2.14	0.746
Phenomenological	15.677	18.56	1.79	0.717

the value of a_s obtained in the LGM is very close to this value. Last, we find the agreement between the phenomenological liquid-drop parameters and the LGM parameters very satisfying.

IV. INFLUENCE OF ISOSPIN DEPENDENT BONDS AND COULOMB FORCE

In this section we present the results of our calculations on the role of the isotopic spin dependence of the interaction strengths and that of the Coulomb force on several observables in the framework of the LGM. We employ the METROPOLIS sampling technique for event generation including the appropriate Coulomb interactions among the protons located at different lattice sites.

For finite nuclei at finite temperature how important is the feature that ϵ_{np} is different from ϵ_{nn} and that there is a Coulomb interaction? One measure is how much the one-body densities ρ_n and ρ_p are sensitive to these effects. Here ρ_n is the one-body neutron density and ρ_p is the one-body proton density. One might attempt to get this from mean-field theories but these give grossly wrong answers [8] and we compute these averaging over events generated by Monte Carlo simulations. In each event the center of mass of the fragmenting system is computed and the density is calculated as a function of distance from it. An unoccupied box has zero density throughout the box and an occupied box has density ρ_0 throughout the box, ρ_0 being the normal nuclear matter density. The density is usually very rugged in an event. A

smoother density results after the canonical ensemble averaging. This is the ‘‘exact’’ one body density we are seeking.

In Fig. 1 we show the one-body density for ^{197}Au at a temperature of 5 MeV along a body diagonal. It is clear that for a nucleus of this size the isotopic spin dependence has considerable effect on the one-body density. What is also clear is that the Coulomb interaction is very important. Unfortunately how this difference will affect the production of clusters, the real experimental observable, is hard to guess. However, one can readily understand how the N/Z ratio of the largest cluster with mass a_{max} gets affected. This is shown in Fig. 2 for the disassembling system ^{197}Au . The average value of $\langle Z_{max} \rangle$ (the average value of Z of the largest cluster) of course depends on the temperature used in the simulation. At low temperature $\langle Z_{max} \rangle$ is close to 79 but will drop in value as the temperature gets raised. It is easy to understand that if only one kind of bond is used the $\langle N_{max} \rangle / \langle Z_{max} \rangle$ ratio stays close to that of the disassembling system. With two kinds of bonds but no Coulomb interaction the ratio of $\langle N_{max} \rangle / \langle Z_{max} \rangle$ is driven towards 1 because this is what the symmetry energy term prefers. However, the Coulomb term will drive the largest cluster towards a higher $\langle N_{max} \rangle / \langle Z_{max} \rangle$ ratio.

A host of observables can be used to identify the liquid-gas-type phase transition from intermediate energy heavy ion fragmentation data. Many of them have been computed in the LGM but mostly without the Coulomb interaction [9]. Here we calculate a few of them using two types of bond and Coulomb interaction. Near the phase transition temperature

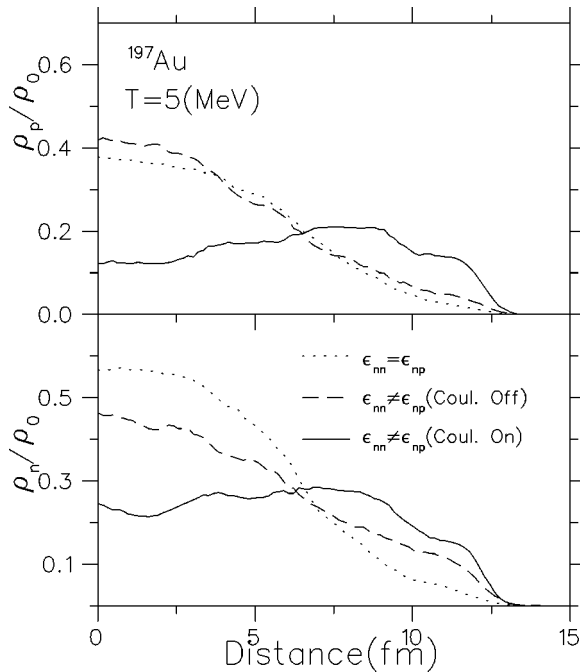


FIG. 1. The proton (upper panel) and neutron (lower panel) one-body densities for ^{197}Au at a temperature of 5 MeV. The dotted lines correspond to calculations with one-type of bond ($\epsilon_{nn} = \epsilon_{pp} = \epsilon_{np} = -5.33$ MeV). The dashed lines represent calculations with two types of bond ($\epsilon_{nn} = \epsilon_{pp} = 0$, $\epsilon_{np} = -5.33$ MeV) without the Coulomb interaction and the solid lines are the same with the inclusion of the Coulomb interaction among the protons.

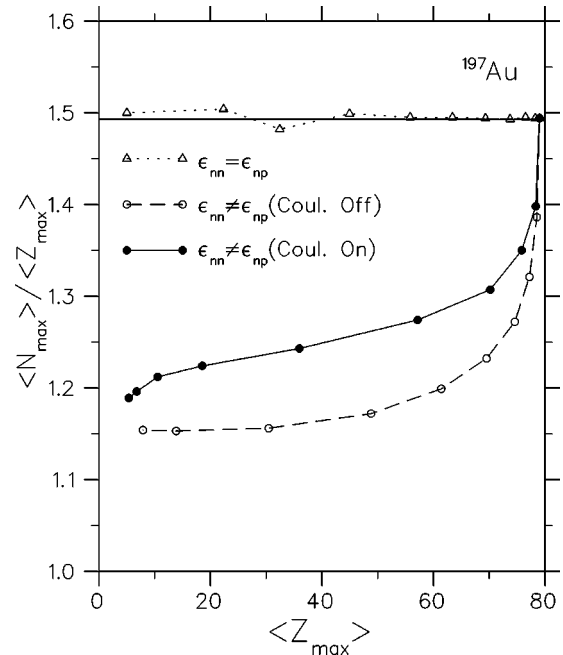


FIG. 2. The evolution of the N/Z ratio of the largest fragment as a function of the atomic number of fragments produced from fragmentation of the ^{197}Au nucleus in the LGM. The different lines have the same meanings as in Fig. 1. The temperature increases by 0.5 MeV between two successive symbols as we move from right to left; the first ones correspond to a temperature 2.5 MeV. The symbol ‘‘ $\langle \rangle$ ’’ stands for the ensemble averaging.

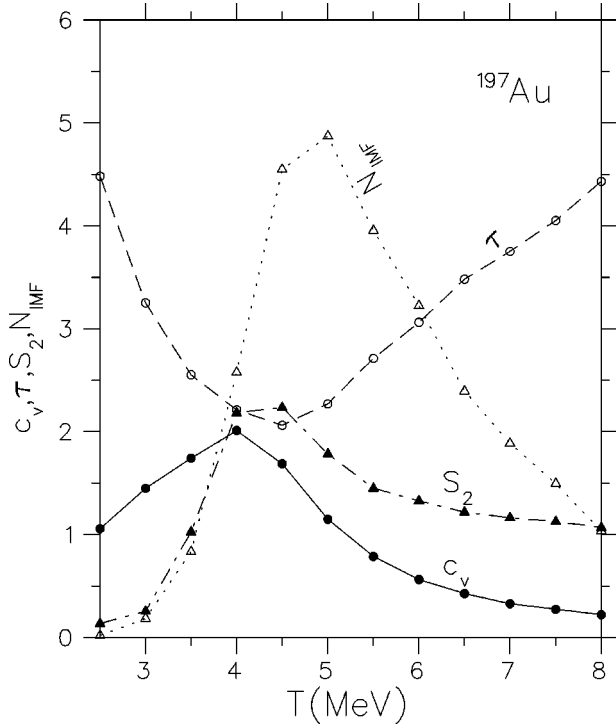


FIG. 3. The specific heat C_v , the exponent τ for the power-law fit to the charge distribution, the second moment S_2 for the charge distribution, and the IMF yield are shown as a function of temperature for fragmentation of ^{197}Au in the LGM. The calculations are done in a 8^3 lattice with two types of bonds and the Coulomb interaction included.

the yields of particles with charge Z go like $Y(Z) \propto Z^{-\tau}$. In Fig. 3 we plot this exponent τ as a function of temperature when the disintegrating system is ^{197}Au . We take a cubic lattice of size 8^3 which corresponds to a freeze-out density of $0.38\rho_0$. We note that the minimum value of τ is 2.1 which is in close agreement with the experiments [10]. In Fig. 3 we also plot several other quantities for the same system. In heavy ion physics one commonly defines intermediate mass fragments (IMFs) as those which have Z between and including 3 and 20. Experimentally, there is clear evidence that starting from low excitation energy in the disintegrating system N_{IMF} first rises, reaches a maximum, and then falls again. The same behavior is noted in the plot. In the figure we also have shown the value of S_2 , the second moment for charge distributions. As a function of T a maximum is clearly discernible. We also plot C_v as a function of temperature which clearly shows a maximum. In experimental data there is evidence of a maximum in the specific heat [11]. This appears to occur around 5 MeV in temperature. We note that the extrema of different observables shown in the figure occur approximately at the same temperature.

Finally we will highlight the roles that the isotopic spin dependence of the nearest neighbor interaction and the Coulomb interaction play in these computations. As an illustration, in Fig. 4 we plot, for ^{197}Au , τ with temperature for (a) no isospin dependence, (b) isospin dependent nearest neighbor interaction, and (c) case (b) plus the Coulomb interaction. In a shift of the minimum of τ the Coulomb interaction

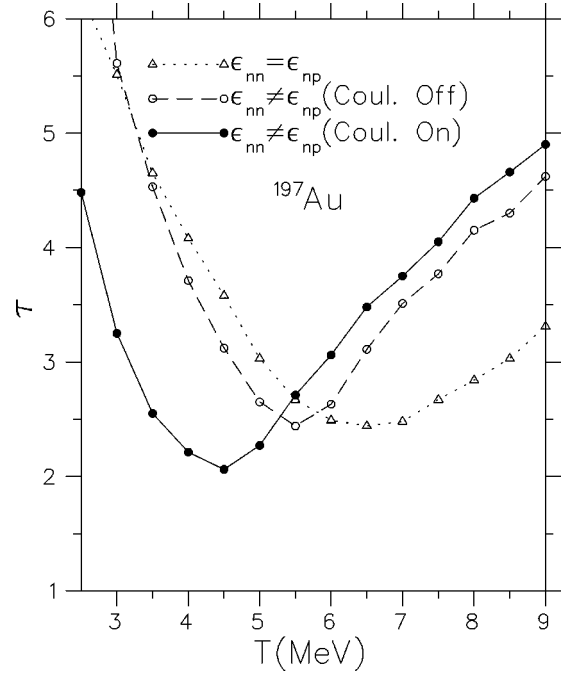


FIG. 4. The exponent τ for the power-law fit to the charge distribution as a function of temperature for fragmentation of ^{197}Au for the cases of (a) no isospin dependence in the nearest neighbor interaction (dotted line with triangles), (b) with an isospin dependent nearest neighbor interaction (dashed line with open circles), and (c) the same as in the case (b) with the Coulomb interaction (solid line with solid circles).

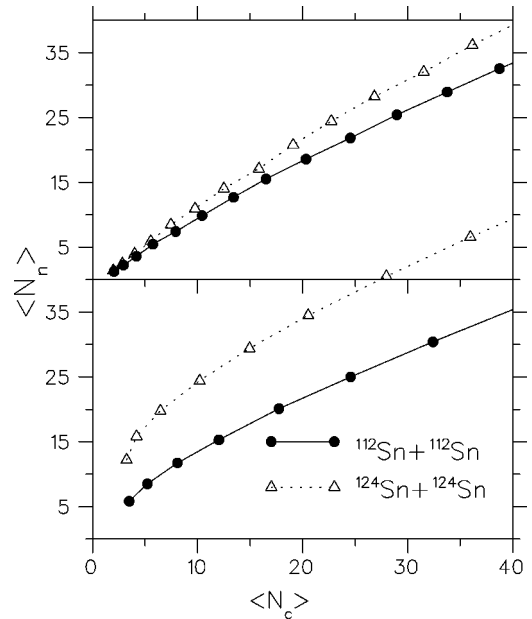


FIG. 5. Correlation between the average number of neutrons and charged particles produced at different temperatures for the reactions indicated. The lowest temperature is 2.5 MeV and T increases by 0.25 MeV between two successive symbols. The upper panel corresponds to calculations with one type of bond and the lower panel represents that with two types of bond including the Coulomb interaction. The calculations are done in a 9^3 lattice.

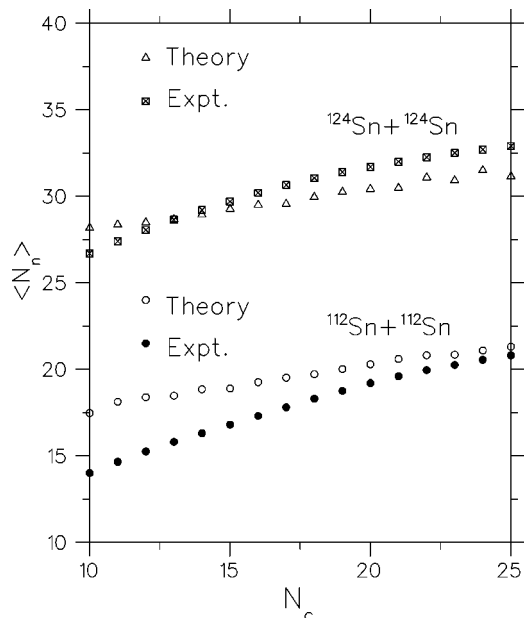


FIG. 6. The same as in Fig. 5 at a fixed temperature $T=3$ MeV with two types of bond (N_c not averaged). The experimental data are also included.

plays a significant role. We verified that as the disintegrating system gets larger with a corresponding growth in the value of Z , the proton number, the minimum of τ , falls to lower and lower temperature, finally disappearing altogether around $Z=120$. It is well known that for central Au on Au collisions there is no minimum in τ [12]. The explanation of this was an early triumph of the LGM with Coulomb interaction.

V. ROLE OF THE ISOSPIN CONTENT OF THE FRAGMENTING SYSTEM ON PARTICLE EMISSION

We have seen above that the isospin dependent LGM reproduces the gross features of intermediate energy heavy ion data. In this section we examine some data which are more exclusive. In an experiment which highlighted the role of the isospin, the average neutron multiplicity was measured as a function of charged-particle multiplicity in $^{124}\text{Sn} + ^{124}\text{Sn}$ and $^{112}\text{Sn} + ^{112}\text{Sn}$ collisions [13]. For example, in the experiment, on the average, about 33 neutrons are emitted in $^{124}\text{Sn} + ^{124}\text{Sn}$ collisions but only about 21 in $^{112}\text{Sn} + ^{112}\text{Sn}$ collisions when the charged multiplicity is 25. In Fig. 5 our calculations for $\langle N_n \rangle$ against $\langle N_c \rangle$ for the two collisions once without any isotopic spin dependence and once including isotopic spin are shown. We input different temperatures to change the average charge-particle multiplicities $\langle N_c \rangle$ and at each temperature we calculate the average neutron multiplicity $\langle N_n \rangle$. This of course does not correspond to the experimental situation identically. To correspond to the experimental situation additional assumptions need to be invoked, like variation of temperature with impact parameter, etc. However, it is clear that an isotopic spin dependent LGM is needed to explain the data. In Fig. 6 we fix temperature at 3

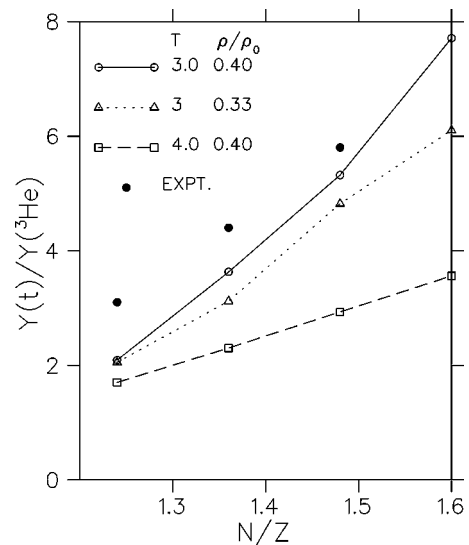


FIG. 7. The ratio of yields of triton to ^3He as a function of the neutron (N) to proton (Z) ratio of the fragmenting system. The different curves correspond to different temperatures and freeze-out densities as indicated in the figure.

MeV and assume that all N_c 's between 10 and 25 arise from this temperature. We then compare the calculations with the data. Here also, in actuality, other temperatures arising from different impact parameters will also contribute to these N_c 's, but at least there are no obvious large contradictions between the data and the isotopic spin dependent LGM.

This calculation also highlights one of the advantages of the LGM. Since the PD recipe gives only particle stable nuclei, calculation of emitted neutrons is straightforward. This is, for example, not true in the Copenhagen statistical model [6] or other types of thermodynamic models [14]. Indeed in these models it is very difficult to compute the number of neutrons since they will largely arise from decay of particle unstable nuclei.

Recently experimental measurements have been performed [15] on the ratios of mirror nuclei emitted from systems with different N/Z values. These data offer a direct test for the isotopic spin dependent part of the LGM. We refer back to Fig. 2 where for ^{197}Au we have shown the N/Z of the largest cluster. The results are significantly different whether we use one kind of bond (no isotopic spin dependence) or two kinds of bonds. This is easily understandable as with proper isotopic spin dependence the largest cluster is driven towards $N/Z=1$ (the Coulomb interaction will slightly compensate this as the Coulomb interaction drives the ratio to values higher than 1). A corollary follows. For the rest of the system, i.e., ^{197}Au -largest cluster, the N/Z ratio is much larger than that of ^{197}Au . Measured $Y(n)/Y(p), Y(t)/Y(^3\text{He})$, etc. (Y referring to the yield of an isotope), will reflect the high N/Z of this remaining system. Therefore the ratio of free neutrons to free protons (monomers) or tritons to ^3He is expected to be higher than that of the dissociating system. In a schematic calculation without the Coulomb interaction this is also noted in Ref. [4].

We test this idea by doing a calculation on an 8^3 lattice. We expect the ratio $Y(t)/Y(^3\text{He})$ to be dependent upon the

input N/Z , the temperature, and possibly the freeze-out density. We expect (also verified numerically) the ratio to be much less dependent on the actual number $N+Z$. We therefore fix N and Z by imposing an N/Z value and $\rho/\rho_0=(N+Z)/N_s=0.4$ and 0.33 . Without any isotopic spin dependence the ratios are indistinguishably the same as the input N/Z but the ratios are much higher with an isotopic spin dependent LGM. This is shown in Fig. 7. In the same figure we also plot the experimental ratios obtained from the reactions $^{112}\text{Sn}+^{112}\text{Sn}$, $^{112}\text{Sn}+^{124}\text{Sn}$, and $^{124}\text{Sn}+^{124}\text{Sn}$ [15]. We note that the experimental ratios are significantly higher than the calculated ones even for the parameter set used giving the closest agreement (solid line), particularly for the lowest N/Z ratio. In our calculations we have assumed that the fragmenting system has an N/Z ratio equal to that of the initial system. Preequilibrium emission may enhance this ratio which may, at least partly, be the cause for this discrepancy at low values of N/Z . In the LGM shell effects are missing. However, it is expected that the shell effects are largely canceled out for the ratio of the yields of mirror nuclei. We again want to emphasize that such an observable is very difficult to cal-

culate in a standard thermodynamic model because many tritons and ^3He will arise from decay of hot nuclei.

In summary, the lattice-gas model with isospin dependent interaction and with the Coulomb interaction describes many features as observed in intermediate energy heavy ion collisions. The model may be used to calculate the signatures for the liquid-gas-type phase transition as are likely to occur in such reactions. Also the dependence of particle emission on the isospin content of the disassembling system can, at least qualitatively, be understood in this model.

ACKNOWLEDGMENTS

This work was supported in part by the Natural Sciences and Engineering Research Council of Canada and by *le Fonds pour la Formation de Chercheurs et l'Aide à la Recherche du Québec*. S.K.S. thanks the Physics Department, McGill University, for hospitality during the course of this work. S.D.G. thanks Betty Tsang for generous help in clarification of experimental data. The authors thank Abhijit Majumder for many helpful discussions.

-
- [1] J. Pan and S. Das Gupta, Phys. Lett. B **344**, 29 (1995).
 - [2] J. Pan and S. Das Gupta, Phys. Rev. C **51**, 1384 (1995).
 - [3] J. Pan and S. Das Gupta, Phys. Rev. C **57**, 1839 (1998).
 - [4] Ph. Chomaz and F. Gulminelli, Phys. Lett. B **447**, 221 (1999).
 - [5] N. Metropolis, A. W. Rosenbluth, M. N. Rosenbluth, A. H. Teller, and E. Teller, J. Chem. Phys. **21**, 1087 (1953).
 - [6] J. P. Bondorf, A. S. Botvina, A. S. Ijilinov, I. N. Mishustin, and K. Sneppen, Phys. Rep. **257**, 133 (1995).
 - [7] W. D. Myers and W. J. Swiatecki, Nucl. Phys. **81**, 1 (1966).
 - [8] S. K. Samaddar, S. Das Gupta, J. N. De, B. K. Agrawal, and T. Sil, Phys. Lett. B **459**, 8 (1999).
 - [9] Y. G. Ma *et al.*, Phys. Rev. C **60**, 024607 (1999).
 - [10] C. A. Ogilvie *et al.*, Phys. Rev. Lett. **67**, 1214 (1991).
 - [11] J. Pochodzalla *et al.*, Phys. Rev. Lett. **75**, 1040 (1995).
 - [12] M. D'Agostino *et al.*, Phys. Rev. Lett. **75**, 4373 (1995).
 - [13] G. J. Kunde *et al.*, Phys. Rev. Lett. **77**, 2897 (1996).
 - [14] A. Majumder and S. Das Gupta, Phys. Rev. C **61**, 034603 (2000).
 - [15] H. S. Xu *et al.*, nucl-ex/9910019.